Supplementary Material on the Methodology Part III

Final report on hydrodynamic connectivity of European hake habitats

Final report

Consultant: José C. Sánchez-Garrido

Date: September 15, 2020

Division: Fisheries and Aquaculture Policy and Resources Division (FIA) / Fisheries and Aquaculture Department

Programme/Project Number: GCP/INT/317 EC Year 9 Baby 2

Hydrodynamic connectivity of European hake habitats in the Alboran Sea: patterns and metrics from a regional ocean model

Abstract

A Lagrangian Flow Network (LFN) analysis was carried out to identify the most likely connectivity links between selected habitat patches of European hake (*Merluccius merluccius*) in the Alboran Sea (AS). Our analysis relied on outputs of a high-resolution regional application of the Massachusetts Institute of Technology general circulation model (MITgcm) to the AS. Movements of hake early life stages (ELS) were represented by passive drifters moving horizontally at fixed depths. The numerical simulations indicate that self-recruitment is the most likely link of the LFN with an average value of 247‰ and 291‰ for north and south Alboran, respectively. We also found that ELS of hake can cross the AS from habitat patches of one coast to another with a probability of 10-15‰ in a time period representative of its pelagic larva duration (PLD; ≈ 40 days). In terms of spawning biomass, we estimated from our analysis that around 0.68% and 0.51% of the total spawning biomass in the AS can be transported all the way from north-to-south and south-to-north, respectively. This meridional transport of hake spawning material appears to be mediated by the two anticyclonic gyres typically present in the AS. The connectivity chance between the Atlantic boxes of the LFN (off Cadiz and Arcila) and those in the AS was estimated in 4.4‰ overall. This link was mainly accounted for the box off Arcila (7.9‰) rather than for the one situated off Cadiz (0.9‰). Our analysis also identified "forbidden" pathways of our network: the Atlantic boxes are isolated from each other, and ELS never reach the Atlantic from the AS. These two constraints are explained by the permanent presence of the swift Atlantic current through the Strait of Gibraltar (the so-called Atlantic jet). Lastly, analysis of sensitivity runs indicate that either increased drifting depths or shorter PLD result in better chances for ELS to cross the AS; whereas these same conditions make it more difficult the input of ELS from the Atlantic. While our analysis indicates that northern and southern habitat locations of hake in the AS are not hydrodynamically isolated from each other, it is uncertain whether the flux of spawning material from one location to another suffices to establish an actual biological link between hake subpopulations at both sites of the basin.

Contents

1. Introduction

The dispersal of marine organisms is largely mediated by the drift of early life stages (i.e., spore, egg, and larva; hereinafter ELS). Under favorable conditions, ELS can travel far enough to reach and eventually thrive within another habitat patch, thereby establishing hydrodynamic connectivity with a second subpopulation. The concept of population connectivity and the corresponding evaluation tools and methods is attracting increasing attention due to its applications in the field of fisheries management and conservation of marine biodiversity (Cowen and Sponaugle, 29).

In order to investigate the stock distribution of European sardine (*Sardina pilchardus*), European hake (*Merluccius merluccius*), and blackspot seabream (*Pagellus bogaraveo*) populations in the Alboran Sea (AS), the Food and Agriculture Organization (through the COPEMED II Project), in collaboration with the General Fisheries Commission for the Mediterranean and the Spanish Institute of Oceanography, promoted the TRANSBORAN Project ("*Transboundary population structure of Sardine, European hake and Blackspot Seabream in the Alboran Sea and adjacent waters: a multidisciplinary approach"*) (Hidalgo et al., 2019). One of the tasks committed in TRANSBORAN is to assess the hydrodynamic connectivity of selected habitat patches for the mentioned fish species. This approach, based on the numerical simulations of ocean currents and the drift of fish ELS, has been broadly used in the fisheries oceanography literature (Dubois et al., 2016; Monroy et al., 2017) and has been already applied in the framework of TRANSBORAN for sardine and blackspot seabream (Sánchez-Garrido, 2018a, b; Sammartino et al. 2019a, b). The present consultancy is intended for the European hake, the third target species in TRANSBORAN.

2. Methods

2.1 Lagrangian Flow Network (LFN) analysis

The methodology employed here combines numerical model simulations and a Lagrangian Flow Network (LFN) analysis procedure applied to the numerical results (Dubois et al., 2016; Monroy et al., 2017). The LFN analysis relies on calculations of ELS's drift trajectories to evaluate the connectivity between selected habitat patches. These habitat patches typically correspond to recognized spawning and nursery grounds of the target species (hake in the present case) and are referred to as "boxes" in LFN

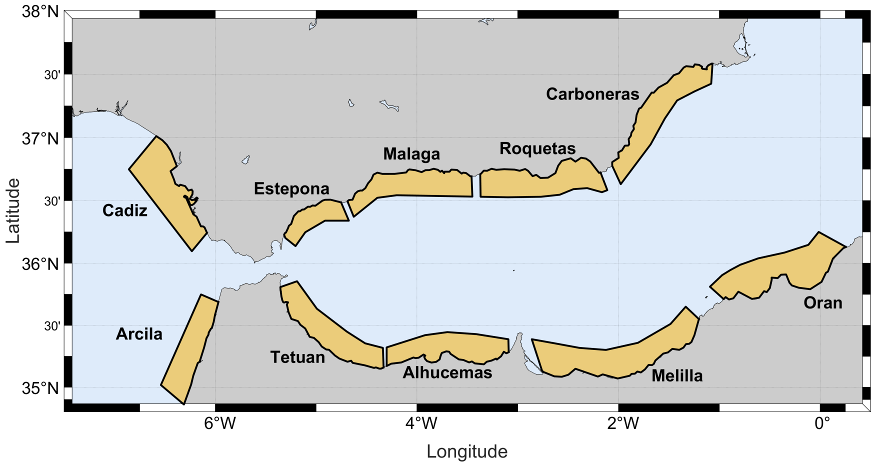

Figure 1. Selected boxes for the LFN analysis.

terminology. In this work we consider a total number of 10 boxes for hake, distributed across the AS (8 boxes) and the Gulf of Cadiz (2 boxes) (Figure 1). These areas were defined after personal communications with Dr Manuel Hidalgo and Dr Alberto García, fisheries experts from the Spanish Institute of Oceanography.

2.2 Regional ocean model

We used the regional application of the Massachusetts Institute of Technology general circulation model (MITgcm; Marshall et al. 1997) developed by Sánchez-Garrido et al. (2013, 2015) to simulate the circulation of the Gulf of Cadiz and the AS. The ocean model is three-dimensional, high-resolution (500 m approx. in the Strait of Gibraltar and 1-2 km in the AS) and is driven by realistic tidal and atmospheric forcing (surface momentum and heat fluxes). For a detailed description of the model, the reader is referred to the papers mentioned above.

The simulation preformed here covers one spawning season of hake (April-to-May; Hidalgo et al. 2009). Model forcing were extracted from larger-scale ocean and atmosphere reanalysis products corresponding to the year 2005. Analysis of a single spawning season allows for the identification of general connectivity patterns in the region. Numerical calculations were carried out in two steps. In the first step, the ocean model was run and its outputs (sea surface height, sea water temperature, salinity, and current velocity) were stored periodically. After examination of the model results (i.e., validation), in the second step the velocity fields from the model (stored every 30 min) were introduced as inputs of a particle tracking algorithm (Sammartino et al. 2018) to simulate the drift of hake ELS. Some of the obtained trajectories are shown in Figure 2.

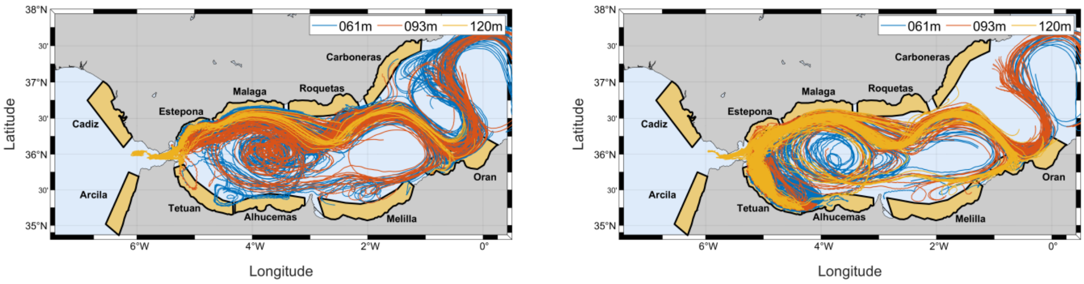

Figure 2. Some ELS trajectories initially released in Estepona (left panel) and Tetuan (right panel) at 61 m (blue lines), 93 m (red lines) and 120 m (yellow lines).

2.3 Lagrangian calculations

Movements of hake ELS were represented by inert particles (drifters) driven by horizontal ocean currents (we assumed ELS have not the ability to swim assumed). Because hake larvae are typically found within 60-120 m depth in the field (Olivar et al. 2003; Sabatés, 2004; Rodríguez et al., 2015), we used ocean currents over this rage of depths to compute ELS trajectories. More specifically, we chose the depths 61 m, 93 m, and 120 m —corresponding to vertical levels 12, 15, and 17 of the model, respectively—.

ELS were tracked in space during a time period representative of the pelagic larva duration (PLD) of hake. We chose 40 days as reference PLD following Hidalgo et al. (2009, 2019). Additional runs with 10 days shorter and longer PLDs (i.e., 30 and 50 days) were conducted to account for the effect of uncertainties of this parameter on our results.

Batch	Release time	PLD (days)	Depth (m)	Remark
#1	April 08, 2005 (23:15 h)	30, 40, 50	61, 93, 120	Flood Tide & Spring Tide
#2	April 09, 2005 (04:45 h)	30, 40, 50	61, 93, 120	Ebb Tide & Spring Tide
#3	April 17, 2005 (05:15 h)	30, 40, 50	61, 93, 120	Flood Tide & Neap Tide
#4	April 17, 2005 (10:45 h)	30, 40, 50	61, 93, 120	Ebb Tide & Neap Tide
#5	April 25, 2005 (11:45 h)	30, 40, 50	61, 93, 120	Flood Tide & Spring Tide
#6	April 25, 2005 (17:15 h)	30, 40, 50	61, 93, 120	Ebb Tide & Spring Tide
#7	May 01, 2005 (17:15 h)	30, 40, 50	61, 93, 120	Flood Tide & Neap Tide
#8	May 01, 2005 (22:45 h)	30, 40, 50	61, 93, 120	Ebb Tide & Neap Tide

Table 1. Lagrangian experiments carried out for every box in the LFN. From left to right: batch number, release time 'month day, year (hour: minute)', PLD, drifting depth (meters), and tidal conditions.

ELS were released within the LFN boxes at 8 different moments in time (Table 1). Released times were selected so as to cover the whole spawning season as well as a broad range of tidal conditions (tides are the main source of flow variability in the Strait of Gibraltar and so can potentially modulate the connectivity between Atlantic and AS boxes). A total of 1,000 ELS were released in each box in every batch, yielding a total number of 240,000 (= 8 × 10 × 10 × 3) trajectories.

3. Results

3.1 Ocean circulation

The simulated surface circulation of the AS (Figure 3) shows well-known features described in the literature (Sánchez-Garrido et al. 2013; Brett et al. 2020): the jet of Atlantic water entering the AS through the Strait of Gibraltar and two large-scale anticyclonic gyres, the Western Alboran Gyre (WAG) and the Eastern Alboran Gyre (EAG). This two-gyre structure is particularly clear in April and May. The system evolves to a one-gyre structure by the end simulation (June-July) as the WAG migrates east and partially merges together with the EAG. Such migration event has been previously documented in the literature (see, e.g., Vélez-Belchí et al. 2005, Flexas et al. 2006).

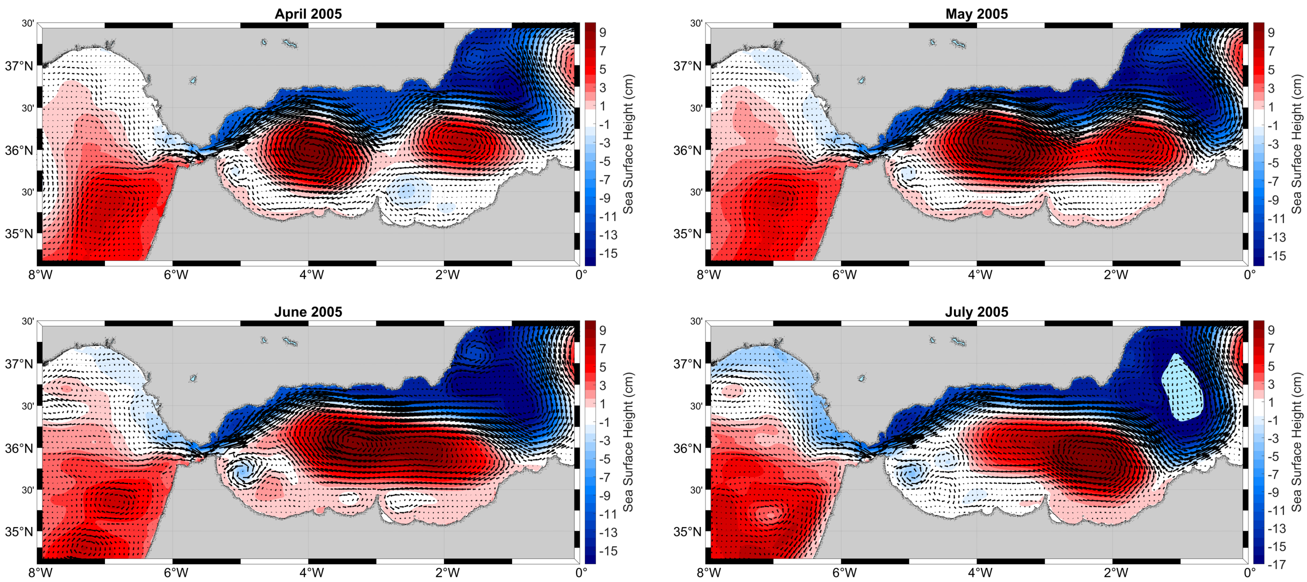

Figure 3. Simulated surface circulation of the Gulf of Cadiz-Alboran Sea region during April-July 2005 (monthly means). The colormap represents sea surface height above datum. Arrows represent sea surface currents.

In our analysis of the trajectories, it is interesting to examine the circulation of the AS over the range of depths at which ELS are situated (61-120 m). Figure 4 shows that the surface circulation pattern is not much distorted with depth, although ocean currents weaken significantly. This is especially true along the northern coast of the AS where the Atlantic jet can be distinguished at 61 m depth (U≈0.5 m/s) but not at 120 m depth (U≈0.25 m/s). A typical velocity magnitude in the AS, U≈ 0.3 m/s, anticipates that hydrodynamic connectivity between the habitat patches of hake could be possible. This statement stems from the inequality $L \leq UT$, where $L \approx$ 500 km is a typical spatial scale of the AS and $T \approx$ 40 days is a PLD for hake.

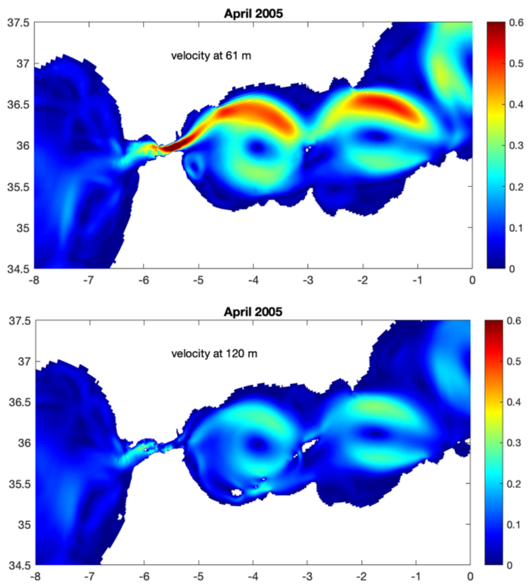

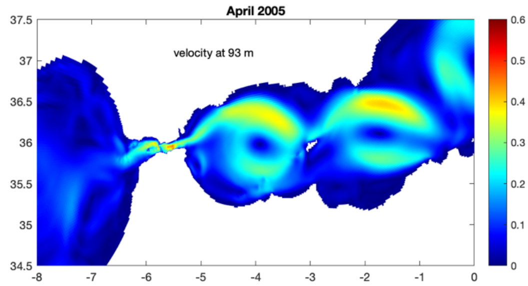

Figure 4. Simulated current velocity at 61, 93 and 120 m depths during April 2005 (monthly means; in m/s).

3.2 Mean connectivity matrix

A mean connectivity matrix from all the computed ELS trajectories (over all PLDs, release times, and drifting depths) provides a global connectivity pattern of our network (Figure 5). The greatest values of connectivity (in ‰) are found in the diagonal of the matrix, indicating that ELS tend to stay and recirculate within its initial box rather than come into another. In other words, self-recruitment, with an average probability of 414‰, is quite likely in every box of the network. The highest self-recruitment value is attained in Cadiz (869‰), whereas the smallest corresponds to Estepona (260‰). Our results also indicate that values of self-recruitment are relatively less variable than other links of the network (see *CV* in the right panel of Figure 5).

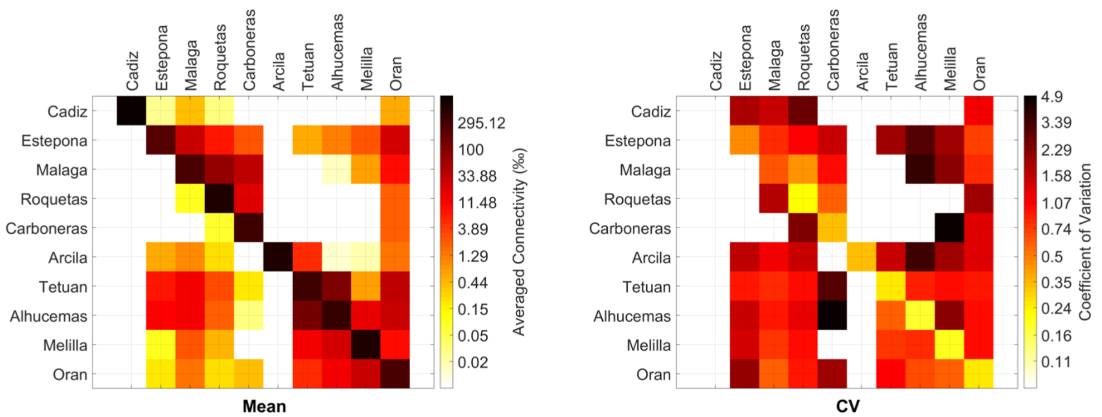

Figure 5. Left: mean connectivity matrix (in ‰) for the whole set of ELS trajectories (see Table 1). Right: Coefficient of Variation (CV) for each element of the connectivity matrix.

Sources and sinks of our network were identified from the relative value of inputs and outputs of ELS for each box (excluding self-recruitment). The two Atlantic boxes, Cadiz and Arcila, do not receive ELS from any other box of the network, but provide ELS to others (0.94‰ and 8.8‰ of their ELS, respectively; Table 2). Hence, these two boxes are pure sources. Other sources of the network —boxes in which outputs exceed inputs— are Estepona, Malaga, Tetuan, and Alhucemas. Sinks of the network are Roquetas, Carboneras, Melilla, and Oran. The major sinks are Roquetas (54‰ input vs 2.2‰ output) and Oran (110‰ input vs 48‰ output). The fact that the two major sources (Cadiz and Arcila) and sinks (Roquetas and Oran) are respectively found in the western and eastern boundaries of our domain is consistent with ELS being carried by prevailing eastwards currents, largely associated with the Atlantic jet (Figure 3 and Figure 4).

	Cadiz	Estep.	Malaga	Roquet.	Carbon.	Arcila	Tetuan	Alhuc.	Melilla	Oran
Input	0	20.48	58.63	89.16	54.03	0	147.33	142.92	47.46	110.25
Output	0.93	62.90	116.48	22.54	2.24	7.98	167.	196.46	45.77	47.96

Table 2. Input and output of ELS for each box of the LFN (in ‰ of their initials ELS).

Because the Atlantic jet flows primarily though the Northern edge of the AS (Figure 3 and Figure 4), west-to-east advection of ELS becomes more obvious in boxes of northern Alboran. For example, the Estepona box does not receive ELS from any other box located at its east (neither from Malaga, Roquetas, nor Carboneras); and the same is true for Malaga. This pattern is not found in any box of southern Alboran, which can all exchange ELS with its western and eastern neighboring boxes.

3.3 Connectivity between macro regions

Based on the mean connectivity matrix we can derive patterns of connectivity between macro-regions of our network (combination of boxes). The following regions are considered: Atlantic (Cadiz and Arcila; North and South Atlantic, respectively), North Alboran (Cadiz, Estepona, Malaga, Roquetas, and Carboneras), and South Alboran (Tetuan, Alhucemas, Melilla, and Oran). Self-recruitment for these regions is calculated from the average mean of the individual self-recruitment percentages of the boxes involved, yielding 692‰ for the Atlantic, 247‰ for North Alboran, and 291‰ for South Alboran.

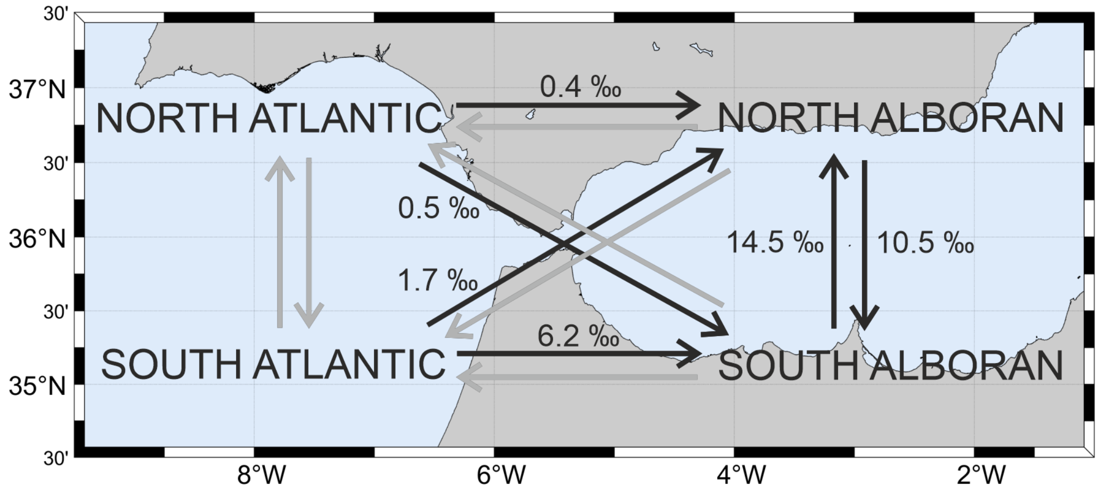

Figure 6. Mean connectivity links between macro-regions of the network (in ‰): North Atlantic (Cadiz), South Atlantic (Arcila), North Alboran (Estepona, Malaga, Roquetas, and Carboneras), and South Alboran (Tetuan, Alhucemas, Melilla and Oran). Gray arrows represent links with null connectivity.

Similar calculations give a 4.4‰ chance for ELS to travel from the Atlantic to the Alboran (either north of south). This transport turns out to be much more probable to occur from Arcila (7.9‰) than from Cadiz (0.9‰) (Figure 6). The two Atlantic boxes are, however, isolated from each other, as any ELS exiting its box was driven elsewhere in the Atlantic or into the AS.

In the AS, 10-15‰ of the ELS released in boxes of one coast ended up into boxes of the opposite coast (10.5‰ travelling from north to south and 14.5‰ from south to north). Such meridional transport is presumably mediated by the two anticyclonic gyres (WAG and EAG), which by encompassing the whole basin represent a two-way conveyor belt joining the northern and southern coasts of the AS. The likelihoods for meridional transport can be combined with estimates of hake spawning biomass in North and South Alboran to provide more refined estimates of the relative importance of north-to-south versus south-to-north transport of spawning material. Spawning biomass in North Alboran nearly doubles that in the South (65% versus 35%; personal communications with Dr. Manuel Hidalgo), from which as much as 0.68% (=65% × 0.0105) and 0.51% (=35% × 0.0145) of the total spawning biomass in the AS could respectively travel from north-to-south and south-to-north in the basin.

3.4 Sensitivity analysis

3.4.1 Drifting depth

The effect of drifting depth on the connectivity of our network is examined in this Section. The connectivity patterns evaluated for each depth individually (61, 93, and

120 m; Figure 7) reflect the essential characteristics of the mean pattern described above: self-recruitment is the most likely scenario for every box, the Atlantic boxes (Cadiz and Arcila) do not receive ELS from any other location, and north-south exchange of ELS in the AS is possible at all depths. However, some quantitative impacts of drifting depth on connectivity are noted.

Greater drifting depths generally enhance self-recruitment, as shown more clearly in the bar diagram of Figure 8. This result is consistent with the residence time of the LFN boxes becoming longer as a result of weaker currents with depth (Figure 4), favoring retention of ELS. The only boxes in which no clear impact of drifting depth on self-recruitment is found are Tetuan and Alhucemas, where current velocities vary only slightly over 61-120 m (Figure 4). Another singular box is Cadiz. This box is shallower than 93 m and so no sensitivity analysis against drifting depth could be conducted — ELS were only released at the shallowest location z = 61 m—

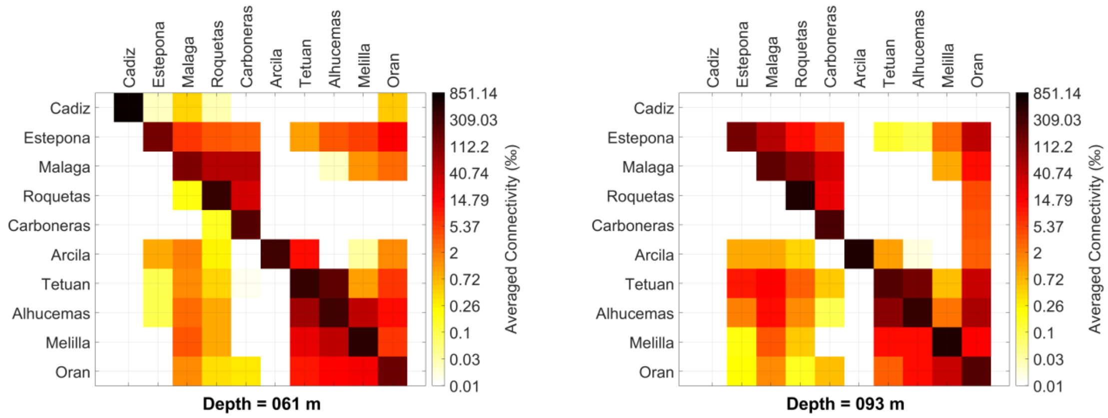

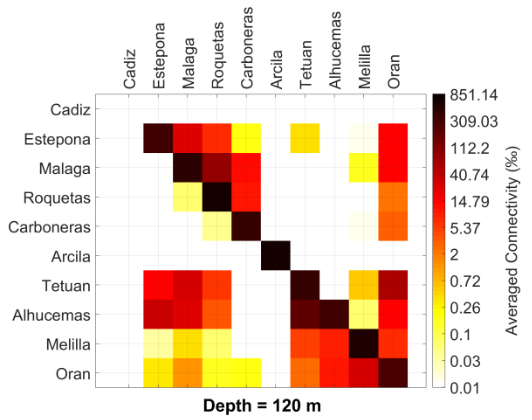

Figure 7. Mean connectivity matrices for 61 m, 93 m, and 120 m drifting depth. Each matrix shows average connectivity values (in ‰) over all PLD (30, 40 and 50 days).

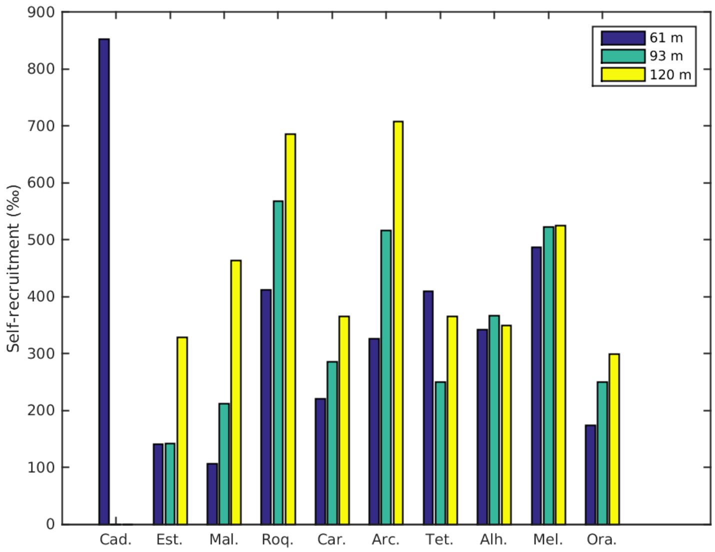

Figure 8. Self-recruitment values for different drifting depths: 61 m, 93 m, and 120 m.

Table 3 shows connectivity values between macro-areas of the LFN (N_{ATL}, S_{ATL}, N_{ALB}, and S_{ALB}) for the three drifting depths analyzed. Because the connectivity between the Atlantic and the AS boxes is mediated by the Atlantic jet, which approximately encompass the surface 100 m of the water column in the Strait of Gibraltar, such connectivity became most likely at the shallowest depth z=61 m, whereas it turned out to be impossible (0‰ probability) at the deepest location z=120 m. In contrast, the connectivity between north and south Alboran, mediated by the WAG and the EAG that extend over much of the water column, was favored at greater depths —especially from south-to-north—. This finding supports the idea that the Atlantic Jet, which is still noticeable at z = 61 m (Figure 4), represents a physical barrier rather than facilitate the crossing of the AS.

Average		N_{ATL}-N_{ALB}	S_{AT} -S_{ALB}	N_{ATL}-S_{ALB}	S_{ATL}-N_{ALB}	N_{ALB}-S_{ALB}	S_{ALB}-N_{ALB}
DEPTH	61 m	**0.5**	**14.6**	**0.6**	**3.0**	6.9	3.0
	93 m	0.0	4.1	0	2.3	**16.2**	12.4
	120 m	0.0	0.0	0.0	0.0	8.5	**28.1**

Table 3. Connectivity values between macro-regions of the network (in ‰). Each row corresponds to mean values for different depths (average mean over all PLDs). Numbers in bold correspond to maximum connectivity values over all depths.

3.4.2 PLD

The connectivity matrices for the different PLDs (30, 40, and 50 days) qualitatively resemble the mean connectivity matrix (Figure 9), and as before (matrices for variable depths) these matrices hold the main connectivity patterns of the LFN described previously. Quantitative impacts of variable PLD on connectivity can be understood from the fact that increased PLD allows for ELS to travel longer distance. Hence, from the perspective of the drifting ELS, the effect is similar of being carried by swifter ocean currents, which in the AS are found towards shallower locations (Figure 4).

Following this reasoning, one could either reduce the drifting depth or make the PLD longer to obtain similar results. The overall decline of self-recruitment probability for longer PLD (Figure 10) supports this idea, although changes of this metric were not particularly strong. Following up with the reasoning, longer PLD generally made more likely the connectivity between Atlantic and AS boxes (as it happened for shallower depths), whereas it reduced the chances of connectivity between northern and southern Alboran, which resulted most likely for the shortest PLD (30 days) (Table 4).

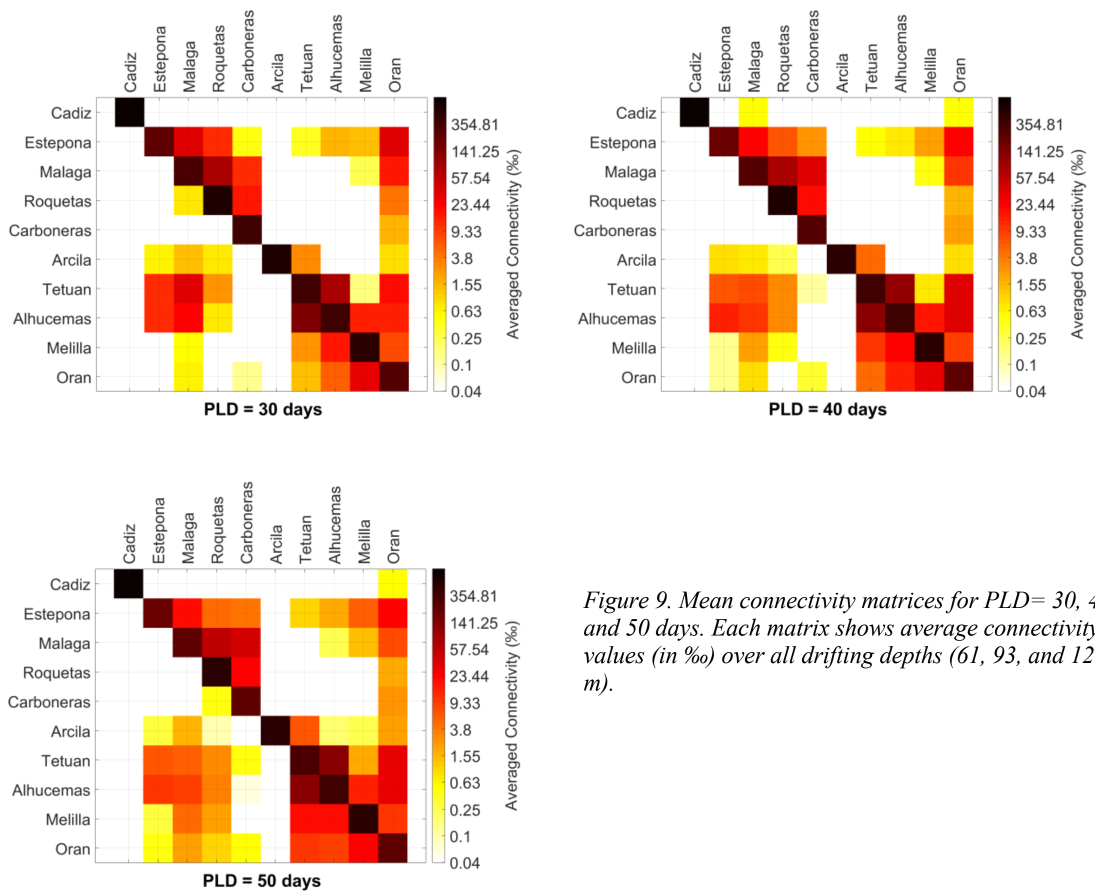

Figure 9. Mean connectivity matrices for PLD= 30, 40, and 50 days. Each matrix shows average connectivity values (in ‰) over all drifting depths (61, 93, and 120 m).

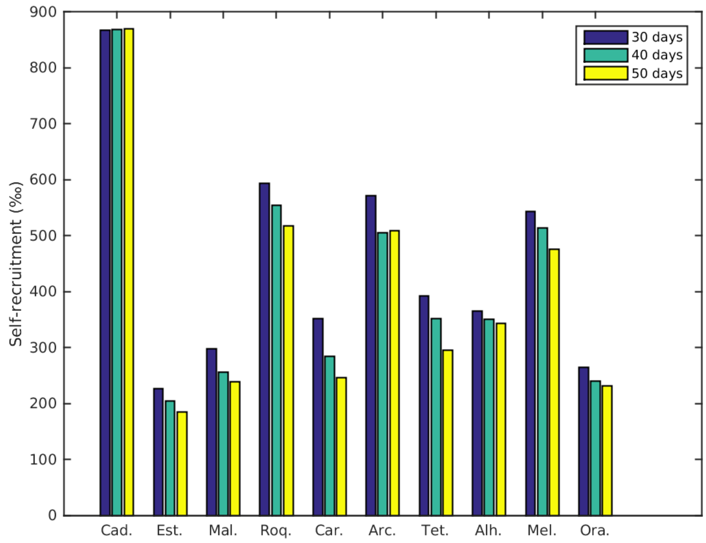

Figure 10. Self-recruitment values for PLD = 30, 40, and 50 days.

Average		NATL-NALB	SATL-SALB	NATL-SALB	SATL-NALB	NALB-SALB	SALB-NALB
PLD	30 days	0.0	4.0	0.0	**2.7**	**15.8**	**21.7**
	40 days	**0.6**	5.6	**0.6**	1.8	10.0	12.1
	50 days	0.0	**9.3**	**0.6**	2.1	10.8	12.4

Table 4. Connectivity values between different macro-regions of the network (in ‰). Each row shows mean values for different PLDs (average mean over drifting depths). Numbers in bold correspond to maximum connectivity values over all PLDs.

3.4.3 Release time

Analysis of the ELS trajectories released in every batch allows for evaluating to what extent the connectivity patterns of our network can change over time. Connectivity patterns can be modified because of the time dependence of the ocean circulation. Our simulation resolves two scales of variability. First, the mesoscale variability (time scales of 10-100 days), notable in the AS as illustrated by the WAG migration event described in Section 3.1 (see also Figure 3). Second, tides. Tidal currents are particularly strong over the continental shelf of the Gulf of Cadiz and in the Strait of Gibraltar and so can potentially regulate the connectivity between the Atlantic and the AS.

Figure 10 shows the connectivity matrices for each ELS batch (8 batches released at different times; see Table 1). North-to-south connectivity in the AS declines from 12.3‰ in the first batch (April 8) to 5.3‰ in the last batch (May 1) (Table 5). This decline is largely due to the interruption of ELS supply from Estepona to Tetuan-Alhucemas (western Alboran), suggesting that the migration of the WAG by the end of the simulation could be its cause. Notably, the south-to-north transport of ELS across the AS remains fairly constant over time (*CV*=0.07), apparently insensitive to changes

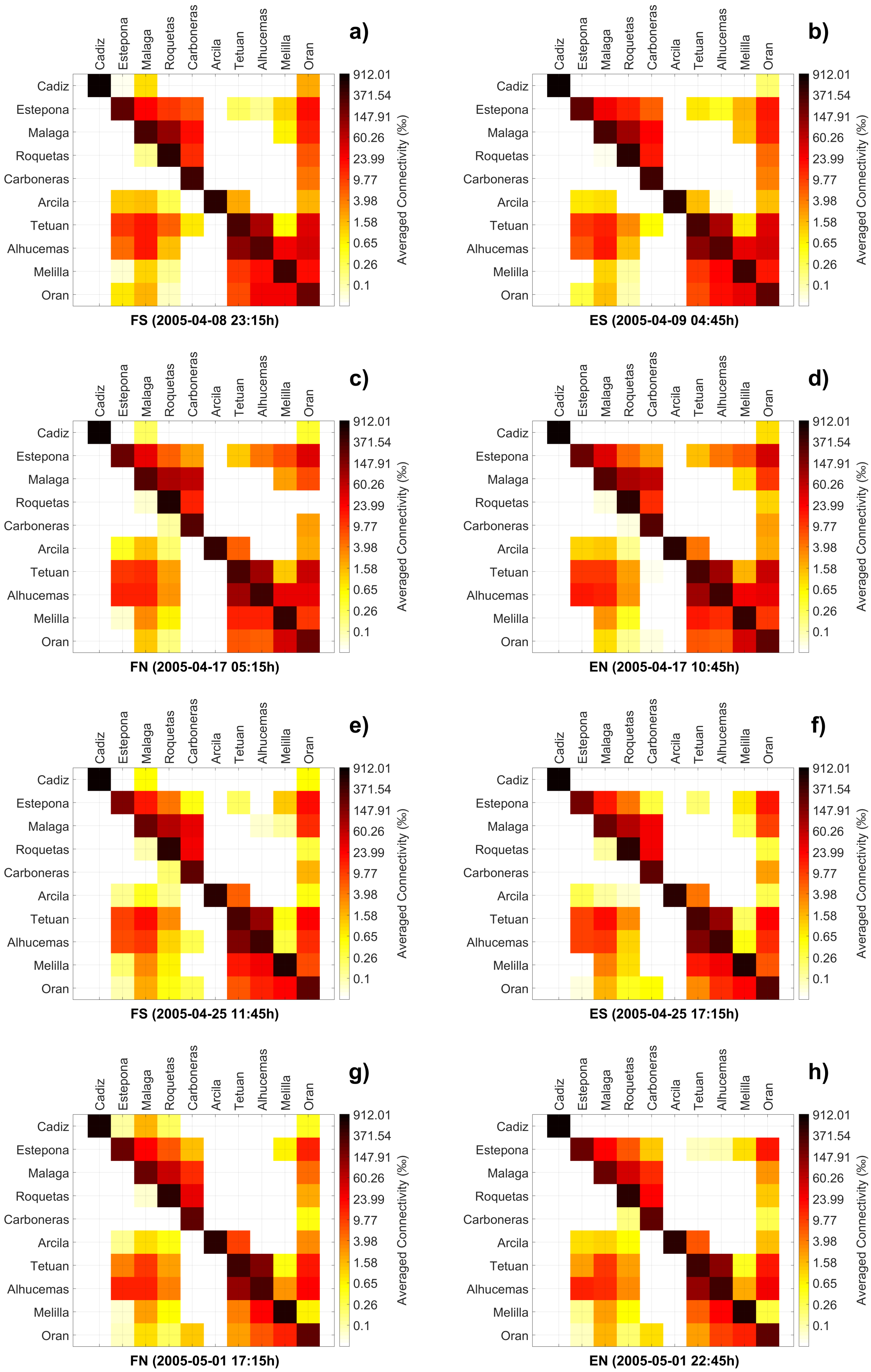

Figure 11 Connectivity matrices for every batch (at different release times). Each matrix shows average connectivity values (in ‰) over all drifting depths (61, 93, and 120 m) and PLDs (30, 40 and 50 days).

in the circulation. Other links subjected to time variability are those between the Atlantic and the AS boxes, especially those involving the North Atlantic box (Cadiz; *CV*>1). Cadiz turns from suppling ELS to other 4 boxes of the network (Estepona, Malaga, Roquetas, and Oran; Fig. 10g) to isolation (zero outputs; Fig. 10h) in batches released only 6 hours apart. Such rapid change supports the idea that the connectivity between the Atlantic and the AS boxes is primarily modulated by tidal currents.

Average		NATL.-NALB.	SATL.-SALB.	NATL.-SALB.	SATL.-NALB.	NALB-SALB	SALB-NALB
Release time	FS (25-04-08 23:15)	0.9	3.6	**1.8**	**2.8**	12.3	14.9
	ES (25-04-09 04:45)	0.0	2.9	0.2	1.8	11.3	14.2
	FN (25-04-17 05:15)	0.2	7.7	0.3	2.0	15.6	**15.6**
	EN (25-04-17 10:45)	0.0	5.9	0.9	2.4	**16.9**	15.5
	FS (25-04-25 11:45)	0.6	6.2	0.6	0.7	8.8	14.7
	ES (25-04-25 17:15)	0.0	4.2	0.0	0.4	7.9	14.6
	FN (25-05-01 17:15)	**1.9**	**11.7**	0.4	1.5	5.9	13.4
	EN (25-05-01 22:45)	0.0	7.7	0.0	2.4	5.3	12.9
Coefficient of Variation		1.50	0.46	1.14	0.48	0.41	0.07

Table 5. Connectivity values between macro-regions of the network (in ‰). Each row shows mean values for different ELS batches (average mean over drifting depths and PLDs). Numbers in bold correspond to maximum connectivity values over all batches.

4. Discussion

The LFN analysis presented here has identified a series of robust links between selected habitat patches of hake distributed in the AS. One of the recurrent features in all the LFN boxes was the relatively high probability of self-recruitment. This result is not completely unexpected, bearing in mind that the boxes in question are situated in coastal regions and therefore feature relatively weak ocean currents in comparison with open waters in the AS. However, most of the self-recruited ELS ended up stuck in the proximity of the model's solid boundaries (onshore), where small-scale processes (boundary layer dynamics, surface waves, etc.) not resolved by the present model can dominate the dynamics. As such, it is possible for the values of self-recruitment presented here to be somewhat overestimated. Dynamical model downscaling in these marginal coastal regions would be necessary to elucidate this question.

A non-null probability for north-south connectivity across the AS (≈10-15‰) was obtained in all the simulations. Although this finding may suggest that mixing between north and south subpopulations of hake would be indeed possible, it should be emphasized that our model does not clarify in which conditions ELS travel, making it difficult to evaluate whether or not the drifting ELS can survive their journey across the AS. For the same reason, weaker links suggested from our model, particularly those between the Atlantic and the AS boxes (e.g., Cadiz <1‰), should be interpreted with particular caution.

Movement of ELS was simulated as simple as possible, exclusively driven by horizontal currents at fixed depths (61, 93 and 120 m). A question that might arise in this regard is what impact of more realistic behavior such as larval diel vertical migrations could have on our results. While additional set of experiments could be carried out to clarify this question, our sensitivity runs partially address this matter, from which the effect of diel vertical migrations can be roughly accounted for the mean average of the connectivity results for different drifting depths.

Lastly, the results presented herein correspond to a single spawning season of hake (year 25). Although the circulation of the AS undergoes interannual variability, this is much weaker that the variability observed at the mesoscale, of which the WAG migration event taking place in our simulation is a good example. Therefore, variations of connectivity values and patterns within the same spawning season (from weak to weak or from month to month) are possibly more significant than yearly variations, and the patterns presented here, particularly the recurrent patterns emerging in every model realization (weak connectivity between Atlantic and AS boxes; no connectivity between the Atlantic boxes; connectivity between north and south Alboran, etc.) are not expected to change substantially from year to year.

5. Conclusions

The main conclusions of this study are the following:

- Self-recruitment is the most likely connectivity scenario for every box of the LFN.
- The Atlantic boxes (Cadiz and Arcila) can export ELS to other locations of the LFN but do not receive ELS from any other box.
- Connectivity within the Atlantic is not allowed.
- Atlantic-to-Alboran connectivity is more likely to occur along the southern coastal margin (7.9‰ versus 0.9‰).

- West-to-east connectivity is only possible between boxes of the AS, not being allowed from the AS to the Atlantic.
- East-to-west connectivity is unlikely between boxes of North Alboran, but it is likely between boxes of South Alboran.
- Connectivity between Northern and Southern AS boxes is relatively likely, with an overall probability of ≈10-15‰.
- Greater drifting depths (within reasonable range) generally increase the chances of connectivity within the AS but reduce the input of ELS from the Atlantic.
- Greater PLDs (within reasonable range) generally decrease the chances of connectivity within the AS and enhance the input of ELS from the Atlantic.
- The connectivity between the Atlantic and the AS boxes is primarily modulated by tidal currents.
- The connectivity between boxes of the AS is primarily modulated by the mesoscale variability of the circulation.

Acknowledgments

This work would have not been possible without the valuable help of Simone Sammartino and Irene Nadal. Discussions with Manuel Hidalgo, Pilar Hernández, Jesús García Lafuente, Alberto García, and Raúl Laiz inspired many contents of this work.

References

Jay Brett, G., L. J. Pratt, I. I. Rypina, and J. C. Sánchez-Garrido (2020) 'The Western Alboran Gyre: an analysis of its properties and its exchange with surrounding water'. J. Phys. Oceanogr., doi: https://doi.org/10.1175/JPO-D-20-28.1.

Cowen, R. K. and Sponaugle, S. (2009). 'Larval dispersal and marine population connectivity'. Annual Review of Marine Science. 1: 443–66.

Dubois, M., Rossi, V., Ser-Giacomi, E., Arnaud-Haond, S., López, C., and Hernández-García, E. (2016). 'Linking basin-scale connectivity, oceanography and population dynamics for the conservation and management of marine ecosystems: Large-scale connectivity and management of marine ecosystems'. Global Ecology and Biogeography, 25(5):503-515

Flexas, M. M., Gomis, D., Ruiz, S., Pascual, A., and León, P. (2006). 'In situ and satellite observations of the eastward migration of the Western Alboran Sea Gyre'. Progress in Oceanography, 70, 486-509.

Hidalgo, M., Tomás, J., Moranta, J., and Morales-Nin, B. (2009). 'Intra-annual recruitment events of a shelf species around an island system in the NW Mediterranean'. Estuarine, Coastal and Shelf Science, 83(2), 227-238.

Hidalgo, M., Rossi, V., Monroy, P., SerGiacomi, E., Hernández-García, E., Guijarro, B., Massutí, E., Alemany, F., Jadaud, A., Pérez, J.L., and Reglero, P. (2019). 'Accounting for ocean connectivity and hydroclimate in fish recruitment fluctuations within transboundary metapopulations'. Ecological Applications, e01913.

Marshall, J., Adcroft, A., Hill, C., Perelman, L., Heisey, C., (1997). 'A finite-volume, incompressible Navier Stokes model for studies of the ocean on parallel computers'. J. Geophys. Res. Ocean. 102, 5753–5766.

Monroy, P., Rossi, V., Ser-Giacomi, E., López, C. and Hernández-García, E. (2017). 'Sensitivity and robustness of larval connectivity diagnostics obtained from Lagrangian Flow Networks'. ICES J. Mar. Sci .74, 1763–1779

Olivar, M.P., Quilez, G. and Emelianov, M. (2003). 'Spatial and temporal distribution and abundance of European hake, *Merluccius merluccius*, eggs and larvae in the Catalan coast (NW Mediterranean)'. Fish. Res. 60, 321–331

Rodríguez, J. M., Cabrero, A., Gago, J., Guevara-Fletcher, C., Herrero, M., Hernandez de Rojas, A. García, R. Laiz-Carrion, A.R. Vergara, P. Alvarez, C. Piñeiro, and F. Saborido-Rey (2015). 'Vertical distribution and migration of fish larvae in the NW Iberian upwelling system during the winter mixing period: implications for cross-shelf distribution'. Fisheries Oceanography, 24(3), 274-290.

Sabatés, A. (2004). 'Diel vertical distribution of fish larvae during the winter-mixing period in the North-western Mediterranean'. ICES J. Mar. Sci. 61, 1243–1252.

Sammartino, S., Sánchez-Garrido, J.C., Naranjo, C., García Lafuente, J., Rodríguez Rubio, P. and Sotillo, M. (2018), Water renewal in semi-enclosed basins: A high resolution Lagrangian approach with application to the Bay of Algeciras, Strait of Gibraltar. Limnol. Oceanogr. Methods, 16: 106-118. doi:10.12/lom3.10231

Sammartino, S. (2019a). 'Connectivity patterns of Blackspot seabream in the Alboran Sea'. Final report'. Transboundary population structure of Sardine, European hake and Blackspot Seabream in the Alboran Sea and adjacent waters: a multidisciplinary approach (0). Framework: COPEMEDII project.

Sammartino, S. (2019b). 'Connectivity patterns of Blackspot seabream in the Alboran Sea'. Final report'. Transboundary population structure of Sardine, European hake and Blackspot Seabream in the Alboran Sea and adjacent waters: a multidisciplinary approach (TRANSBORAN). Framework: COPEMEDII project.

Sánchez-Garrido, J.C., García Lafuente, J., Álvarez Fanjul, E., Sotillo, M. G. and de los Santos, F.J. (2013). 'What does cause the collapse of the western Alboran Gyre? Results of an operational ocean model'. Progress in Oceanography. 116, pp. 142 - 153.

Sánchez-Garrido, J.C., Naranjo, C., Macías, D., García Lafuente, J. and Oguz, T. (2015). 'Modeling the impact of tidal flows on the biological productivity of the Alboran Sea', 120, 7329-7345.

Sánchez Garrido, J.C. (2018a) 'Hydrodynamic Modelling of the Alboran Sea'. Intermediate report. Transboundary population structure of Sardine, European hake and Blackspot Seabream in the Alboran Sea and adjacent waters: a multidisciplinary approach (TRANSBORAN). Framework: COPEMEDII project.

Sánchez Garrido, J.C. (2018b) 'Hydrodynamic Modelling of the Alboran Sea'. Final report. Transboundary population structure of Sardine, European hake and Blackspot Seabream in the Alboran Sea and adjacent waters: a multidisciplinary approach (TRANSBORAN). Framework: COPEMEDII project.

Vélez-Belchí, P., Vargas-Yáñez, M., and Tintoré, J. (2005). 'Observation of a western Alborán gyre migration event'. Progress in Oceanography, 66, 190-210,

Appendix: Mean connectivity matrix

	Cadiz	Estepona	Malaga	Roquetas	Carboneras	Arcila	Tetuan	Alhucemas	Melilla	Oran
Cadiz	868.56	0.02	0.380	0.03	0.00	0.00	0.00	0.00	0.00	0.51
Estepona	0.00	203.85	25.54	7.38	2.59	0.00	0.51	1.17	2.68	23.04
Malaga	0.00	0.00	260.26	75.63	30.47	0.00	0.00	0.01	0.72	9.65
Roquetas	0.00	0.00	0.08	555.12	20.38	0.00	0.00	0.00	0.00	2.08
Carboneras	0.00	0.00	0.00	0.07	290.30	0.00	0.00	0.00	0.01	2.16
Arcila	0.00	0.60	0.92	0.23	0.00	516.28	4.75	0.01	0.02	1.45
Tetuan	0.00	8.22	14.19	3.08	0.17	0.00	341.04	108.22	0.72	32.39
Alhucemas	0.00	11.37	13.73	2.05	0.03	0.00	124.31	352.36	15.31	29.67
Melilla	0.00	0.08	2.42	0.48	0.00	0.00	12.33	21.16	511.16	9.29
Oran	0.00	0.19	1.38	0.22	0.39	0.00	5.43	12.35	28.01	240.64

Mean connectivity matrix (Figure 5; left panel). Values in ‰.